Proceedings of the CAS–CERN Accelerator School: Beam Injection, Extraction and Transfer, Erice, Italy, 10-19 March 2017, edited by B. Holzer, CERN Yellow Reports: School Proceedings, Vol. 5/2018, CERN-2018-008-SP (CERN, Geneva, 2018)

Emittance Preservation

V. Kain
CERN, Geneva, Switzerland

Abstract
The transverse emittance is a critical parameter for the performance of synchrotron light sources, linear and circular colliders, and many other applications. The best performance is often achieved with the smallest emittances. Many effects lead however to emittance growth. In this lecture emittance growth from mismatch at injection into circular machines will be discussed. The concept of emittance and how to calculate it will be introduced and the formulae for emittance blow-up for the most common injection errors will be derived.

Keywords
Emittance; brightness; accelerator performance; emittance blow-up.

1 Introduction

One of the key figures of merit in circular and linear colliders is the collider *luminosity*. It is defined as

$$\mathcal{L} = \frac{N_+ N_- f}{2\pi \Sigma_x \Sigma_y}\,, \tag{1}$$

where $\Sigma_{x,y} = \sqrt{\sigma^{*2}_{x,y+} + \sigma^{*2}_{x,y-}}$ describes the convolution of the colliding particle distributions with horizontal and vertical beam sizes $\sigma^*_{x,y}$ at the interaction point, N_+, N_- the number of particles in the two beams, and f the revolution frequency. In the case of round Gaussian beams and the same distribution for both beams, the formula for luminosity simplifies to

$$\mathcal{L} = \frac{N_+ N_- f}{4\pi \beta^* \varepsilon}\,, \tag{2}$$

where β^* is the β function at the collision point and ε is the emittance of the beam. The luminosity thus depends directly on the emittance in the vertical and the horizontal plane. The smaller the emittance, the higher the luminosity and the higher is the collision rate at the experiment.

As long as the dynamics of the particle beams is governed by conservative forces, the area occupied by the beam in phase space remains constant. We will see later that the area in phase space that is occupied by the beam is related to the emittance of the beam. Many effects exist nevertheless that alter the distribution in phase space. Synchrotron radiation, for example, will lead to a decrease of the emittance. Various beam cooling mechanisms, such as stochastic and electron cooling, are also available in specific circumstances to decrease the beam emittance in a controlled manner. A big class of effects, however, leads to an uncontrolled increase of the emittance. Intra-beam scattering, power supply noise, crossing resonances, beam instabilities, alignment errors, and dispersion for e^- linacs are examples of these issues; another category of emittance growth is due to errors at injection into synchrotrons or linacs, where we typically speak of *mismatch* of various parameters. In this lecture we will discuss how mismatch at injection can introduce emittance blow-up. We will start with a general definition and discussion of emittance and how to calculate it for a given particle distribution. This will then be input to calculate emittances for altered particle distributions due to mismatch. The effects will be explained mostly referring to the horizontal plane. The same considerations can be applied to the vertical plane. The material used for the preparation of these lectures is mainly from Refs. [1–3].

https://doi.org/10.23730/CYRSP-2018-005.345

2 Emittance

For many calculations and applications, the canonical conjugate variable pair called *action-angle variables* (J, ϕ) prove to be a practical concept. The relation between Cartesian (x and x') and action-angle variables in the horizontal plane is given in Fig. 1. It shows the well-known elliptic particle trajectory in horizontal phase space. The area A of the phase-space ellipse is proportional to action J_x via $A = 2\pi J_x$.

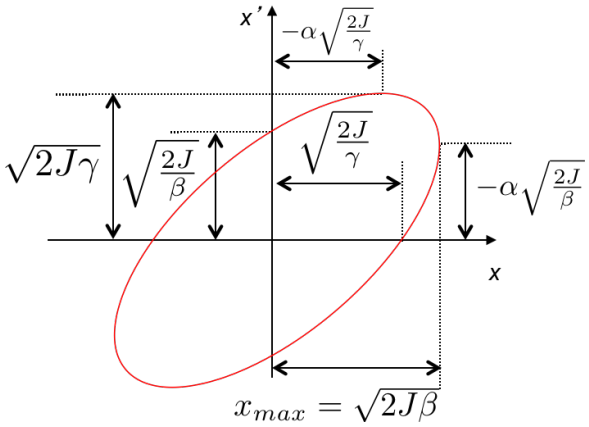

Fig. 1: Phase-space in the horizontal plane. The area of the ellipse defines the action J_x, with $A = 2\pi J_x$

The transformation between action-angle variables and Cartesian variables is summarised in Eqs. (3) and (4). The action J_x is a measure of the particle amplitude of motion, see Eq. (4).

$$\begin{aligned} 2J_x &= \gamma_x x^2 + 2\alpha_x x' x + \beta_x x'^2 \\ \tan\phi_x &= -\beta_x x \frac{x}{x'} - \alpha_x \end{aligned} \tag{3}$$

$$\begin{aligned} x &= \sqrt{2\beta_x J_x}\cos\phi_x \\ x' &= -\sqrt{\tfrac{2J_x}{\beta_x}}(\sin\phi_x + \alpha_x \cos\phi_x)\,. \end{aligned} \tag{4}$$

The advantage of action-angle variables becomes apparent when observing them under symplectic transformations as for example under transfer matrices. Symplectic operations M are defined as

$$M^T \cdot S \cdot M = S \tag{5}$$

where S is defined as

$$S = \begin{pmatrix} 0 & 1 & 0 & 0 & 0 & 0 \\ -1 & 0 & 0 & 0 & 0 & 0 \\ 0 & 0 & 0 & 1 & 0 & 0 \\ 0 & 0 & -1 & 0 & 0 & 0 \\ 0 & 0 & 0 & 0 & 0 & 1 \\ 0 & 0 & 0 & 0 & -1 & 0 \end{pmatrix}. \tag{6}$$

Symplectic operations are phase-space area-preserving, and thus action-preserving, operations. The concept of action-angle variables is also useful for our discussion as it allows to define the emittance in very simple terms. The emittance is defined as the mean action of all particles in the beam:

$$\varepsilon_x = \langle J_x \rangle\,. \tag{7}$$

It is related to the width of the transverse distribution and can hence also be calculated from the second-order moments of the distribution in phase space with the σ-matrix

$$\sigma = \begin{pmatrix} \langle x^2 \rangle & \langle x x' \rangle \\ \langle x x' \rangle & \langle x'^2 \rangle \end{pmatrix} \tag{8}$$

and the emittance as

$$\varepsilon_x = \sqrt{|\sigma|} = \sqrt{\langle x^2\rangle\langle x'^2\rangle - \langle xx'\rangle^2}\,. \tag{9}$$

We refer to this definition as rms-emittance. For phase-space distributions that are centred around 0 in x and x', both definitions, (7) and (9), are equivalent.

3 Mismatch at injection

Injection into a circular accelerator is a delicate process. Imprecise delivery of the beam for instance or mismatch in the optics parameters lead to emittance blow-up and possibly to losses. In the following, the methodology to calculate the emittance blow-up due to injection errors will be introduced for the most important and most typical imperfections. The treatment can then be applied to other problems. Most illustrations and calculations make use of *normalised coordinates*, another practical concept. In normalised phase space the elliptical trajectories from real phase space become circles, see Fig. 2. The transformation from real phase-space coordinates x, x' to the normalised coordinates $\overline{x}, \overline{x}'$ is given in Eq. (10)

$$\begin{pmatrix}\overline{x}\\ \overline{x}'\end{pmatrix} = N\cdot\begin{pmatrix}x\\ x'\end{pmatrix} = \sqrt{\frac{1}{\beta_x}}\cdot\begin{pmatrix}1 & 0\\ \alpha_x & \beta_x\end{pmatrix}\cdot\begin{pmatrix}x\\ x'\end{pmatrix}\,. \tag{10}$$

Whereas the equation of the ellipse for real phase space is,

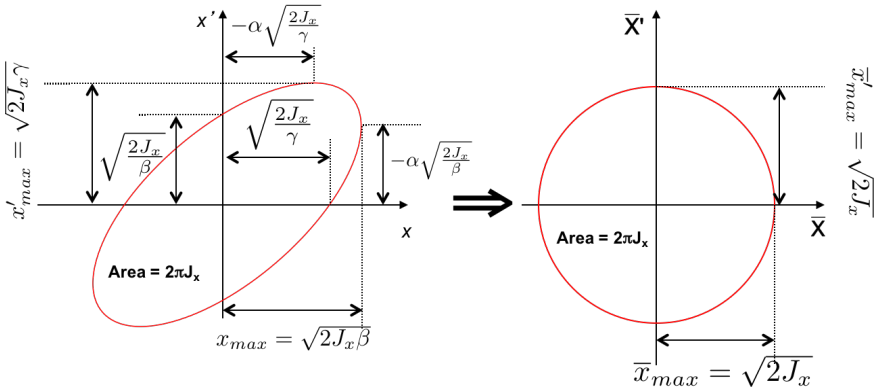

Fig. 2: In normalised phase space the trajectories are circles. The area stays the same and is linked to the action of the particle.

$$2J_x = \gamma_x x^2 + 2\alpha_x p_x + \beta_x p_x^2\,, \tag{11}$$

it becomes the equation of a circle in normalised phase space

$$2J_x = \overline{x}^2 + \overline{x}'^2\,. \tag{12}$$

The area enclosed by the trajectory in real as well as normalised phase space is $A = 2\pi J_x$.

3.1 Steering (dipole) error

If the beam is not injected on the closed orbit as indicated in Fig. 3, i.e., $x \neq x_{CO}$ and/or $x' \neq x'_{CO}$, the injected beam will perform so-called injection oscillations around the closed orbit for several turns until the beam has filamented and the emittance has effectively grown. In phase space at the location of the injection point, a steering error will lead to a particle distribution that is off-centred with respect to the matched distribution as indicated in Fig. 4. In Fig. 5 snapshots of the evolution of the mismatched

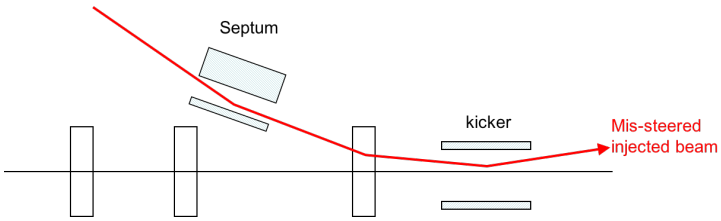

Fig. 3: The injected beam arrives with an offset in position and angle at the injection point. This will result in injection oscillations.

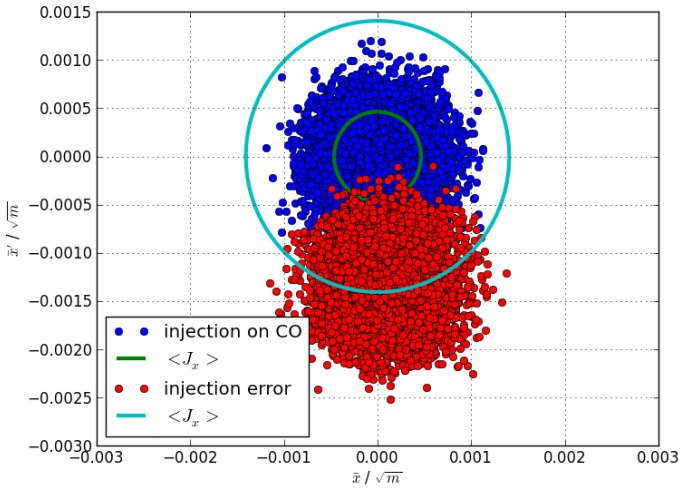

Fig. 4: The blue particle distribution is beam injected without steering error, whereas the red one arrives with an injection angle error. The mean action for both distributions is also indicated.

distribution (red distribution in figure) turn after turn are shown. In this example the particles experience only linear fields and the centroid of the red particle distribution will move on a circular trajectory. The centroid of the distribution is performing *injection oscillations*, as it can be measured turn-by-turn by a single beam position monitor, Fig. 6, while the width of the distribution remains constant, Fig. 7. Figure 8 finally shows the evolution of the emittance turn-by-turn. Injection is supposed to happen at turn 20 in that figure. Both definitions (7) and (9) are applied to the red particle distribution and shown in Fig. 8. Whereas the rms-emittance corresponds to what we see in Fig. 7, the width of the distribution remains constant, the usefulness of the emittance via mean action does not seem apparent. This will be different in the presence of non-linear fields in the circular accelerator, where the particles' tune will depend on their amplitude.

In case of non-linear fields, the area occupied by the particle distribution in phase space will change, Fig. 9. *Filamentation* will take place until the distribution will cover again all phases, see Fig. 10. The projection into the horizontal plane after many turns, as it can be measured by a profile monitor, is shown in Fig. 11. It is no longer Gaussian. Smaller injection errors than in the example just lead to the creation of non-Gaussian tails, a phenomenon which is frequently seen in day-to-day accelerator operation. At the same time as the filamentation occurs, the oscillation amplitude of the centroid will reduce. In fact the oscillation amplitude will decay exponentially following $A(t) = A_0 \cdot e^{-\frac{t}{\tau}}$, where τ is the filamentation time. The *damped* motion of the centroid under the influence of non-linear fields

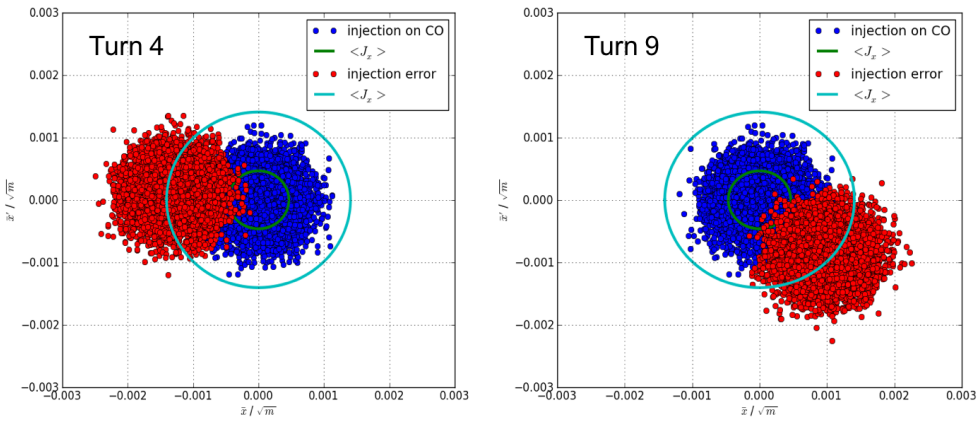

Fig. 5: The centroid of the particle distribution will move on a circular trajectory in normalised phase space turn after turn.

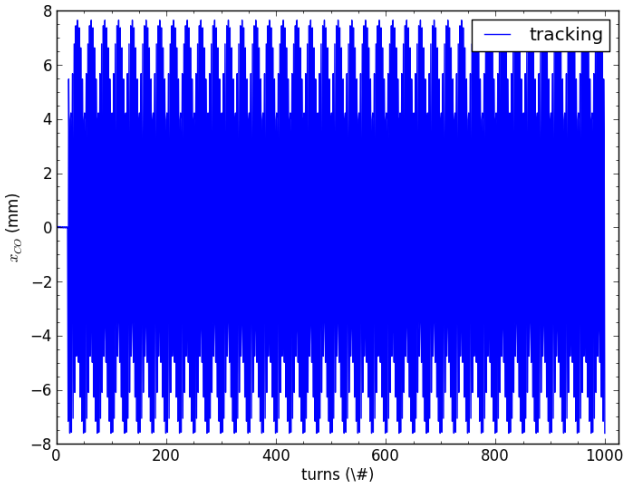

Fig. 6: Turn-by-turn beam position measurements with a beam position monitor reveal *injection oscillations* in case of injection with steering error.

is shown in Fig.12. As before, we can plot the evolution of the emittance using the mean action of the particle distribution and the rms-emittance as defined in (9), see Fig. 13. The important conclusion from the short phenomenological introduction of the effect on the emittance growth from an injection steering error is that the emittance from mean action corresponds to the rms-emittance after full filamentation. Or as said earlier the emittance definition from mean action is equivalent to the rms-emittance in case of a particle distribution where mean angle and position are zero.

This input will now be used to derive the formula to calculate the emittance blow-up for a given injection steering error. A collection of particles is injected with an error in position and angle as indicated in Fig. 14. For an injection error $\Delta a[\sigma]$ in units of $\sigma = \sqrt{\beta\varepsilon}$, the misinjected beam is offset in normalised phase space by $L = \Delta a\sqrt{\varepsilon}$. The particle coordinates of the misinjected beam with respect

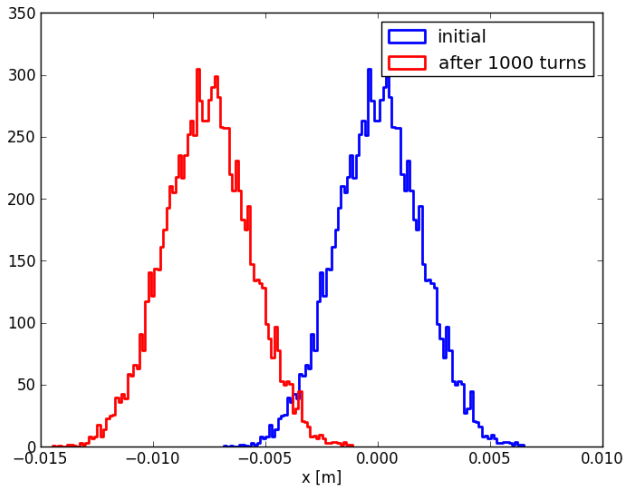

Fig. 7: Horizontal distributions for different turns as could be measured by a turn-by-turn profile monitor. The width of the distribution stays the same, but the mean is changing form turn to turn.

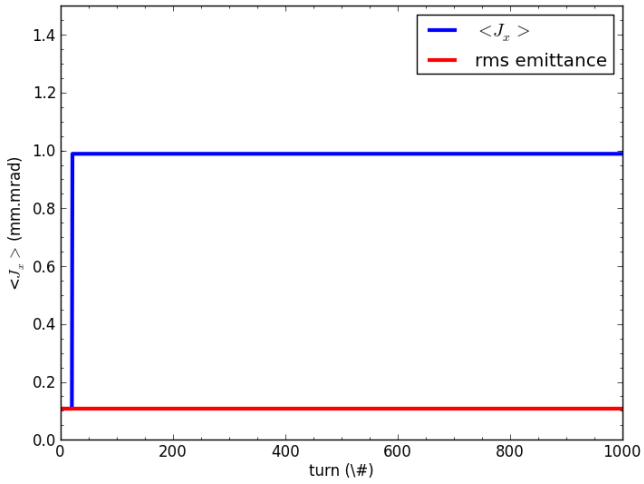

Fig. 8: Evolution of mean action and rms emittance as a function of turn. The injection occurs at the time turn = 20.

to the matched distribution are

$$\begin{aligned} \overline{x}_{new} &= \overline{x}_0 + L\cos\theta \\ \overline{x}'_{new} &= \overline{x}'_0 + L\sin\theta \end{aligned} \tag{13}$$

and the action for one particular particle becomes

$$\begin{aligned} 2J_{new} &= \overline{x}^2_{new} + \overline{x}'^2_{new} = (\overline{x}_0 + L\cos\theta)^2 + (\overline{x}'_0 + L\sin\theta)^2 \\ &= \overline{x}^2_0 + \overline{x}'^2_0 + 2L(\overline{x}_0\cos\theta + \overline{x}'_0\sin\theta) + L^2\,. \end{aligned} \tag{14}$$

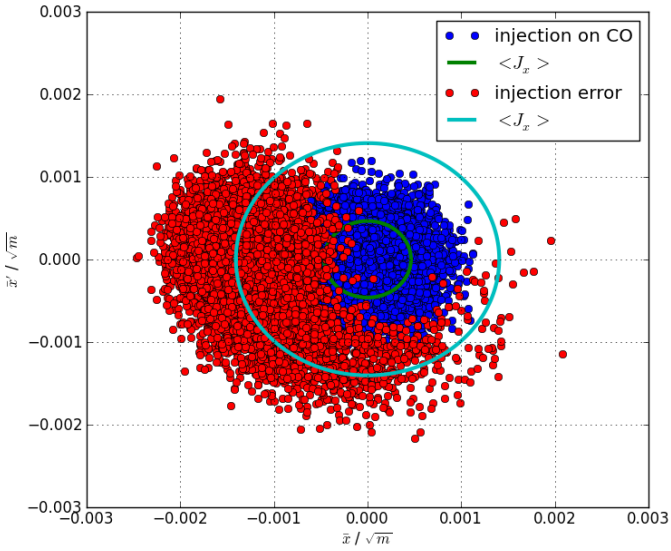

Fig. 9: Particle distribution with injection error in red after 100 turns in the presence of non-linear fields in the circular accelerator. The distribution is filamenting.

For the emittance we need the mean action of all particles:

$$\begin{aligned} 2\langle J_{new}\rangle &= \langle \overline{x}_0^2\rangle + \langle \overline{x}_0'^2\rangle + \langle 2L(\overline{x}_0\cos\theta + \overline{x}_0'\sin\theta)\rangle + L^2 \\ &= 2\varepsilon_0 + 2L(\langle \overline{x}_0\cos\theta\rangle + \langle \overline{x}_0'\sin\theta\rangle) + L^2 \\ &= 2\varepsilon_0 + L^2 \end{aligned} \tag{15}$$

using $\langle\cos\theta\rangle = 0$ and $\langle\sin\theta\rangle = 0$. And the emittance increase is hence

$$\begin{aligned} \varepsilon_{new} &= \langle J_{new}\rangle = \varepsilon_0 + L^2/2 \\ &= \varepsilon_0(1 + \Delta a^2/2)\,. \end{aligned} \tag{16}$$

Equation (16) can also be written for real phase-space coordinates, where Δx and $\Delta x'$ are the errors at injection with respect to the horizontal closed orbit at injection:

$$\frac{\varepsilon}{\varepsilon_0} = 1 + \frac{1}{2}\frac{\Delta x^2 + (\beta\Delta x' + \alpha\Delta x)^2}{\beta\varepsilon_0}\,. \tag{17}$$

As we have seen now, injection oscillations are detrimental for emittance preservation and therefore need to be corrected. Frequently the input for the correction algorithm is not the oscillation measured at a single pick up over many turns, but rather the difference of the first turn trajectory from the injection closed orbit measured with many pick ups. In Fig. 15 an example of the injection oscillation display in the LHC control room is shown. It contains the trajectory reading in the transfer line between the LHC pre-injector and the LHC as well as the injection oscillations in the first 3 km long part of the LHC. The usual trajectory correction algorithms are used to find the best dipole correctors in the transfer line to minimise the injection oscillation amplitudes in the LHC. The horizontal injection oscillation amplitude in the example is 2 mm, corresponding roughly to 2 σ. Let's apply Eq. (16) to calculate the emittance blow-up for $\Delta a = 2\sigma$. According to Eq. (16) the emittance blow-up will be $\varepsilon_{new} = \varepsilon_0(1 + \Delta a^2/2) = 3\varepsilon_0$. For comparison, the allowed emittance growth budget in the LHC is only 10%. Clearly, these injection oscillations would need to be corrected.

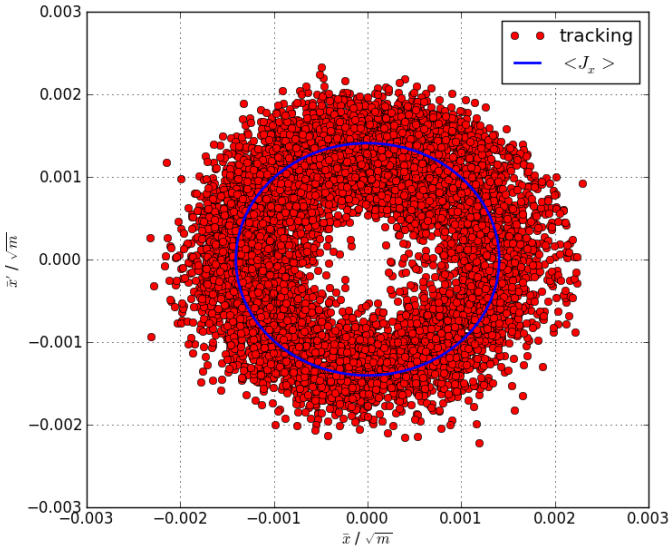

Fig. 10: After filamentation the beam covers all phases in phase space and the area is larger than initially

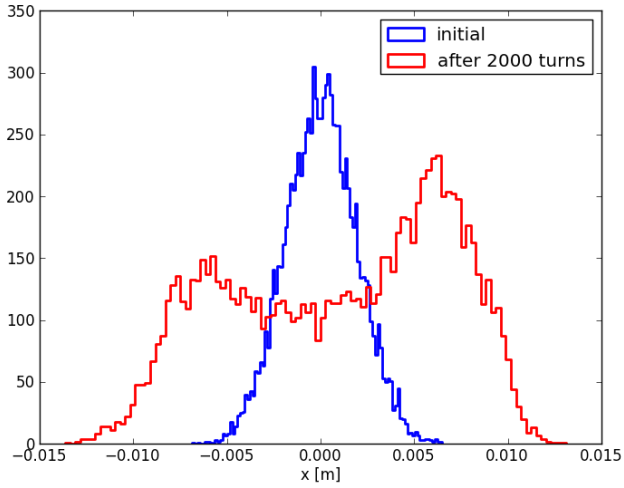

Fig. 11: Filamentation leads to a larger beam size measured at a profile monitor. The distribution has also become non-Gaussian. The mean of the distribution remains constant after filamentation.

The kind of injection oscillation correction discussed so far will however only remove the static contributions to the steering errors. Small variations of the injected trajectory might also occur on a shot-by-shot basis or if the injected beam consists of several bunches, the equipment involved in the transfer might introduce slightly different trajectories and hence different injection oscillations for the different bunches. These injection errors can only be corrected by the transverse feedback system in the receiving circular machine. The feedback damping time needs to be faster than the filamentation time to avoid emittance blow-up.

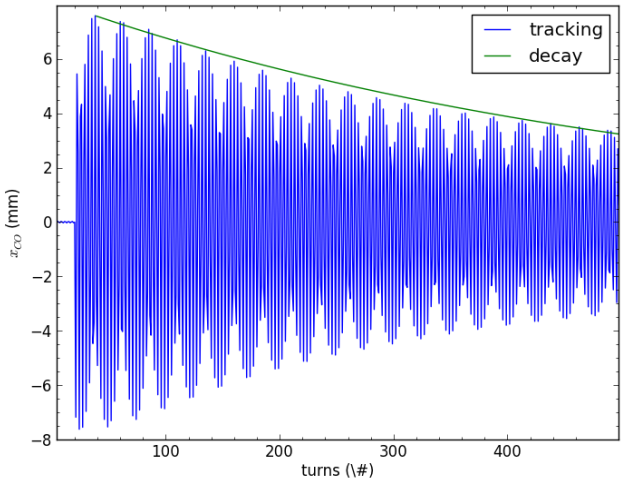

Fig. 12: In the presence of non-linear fields, damping of the centroid motion occurs after an injection error. The decay of the oscillation amplitudes can be fitted with $A(t) = A_0 \cdot e^{-\frac{t}{\tau}}$, where τ is the filamentation time.

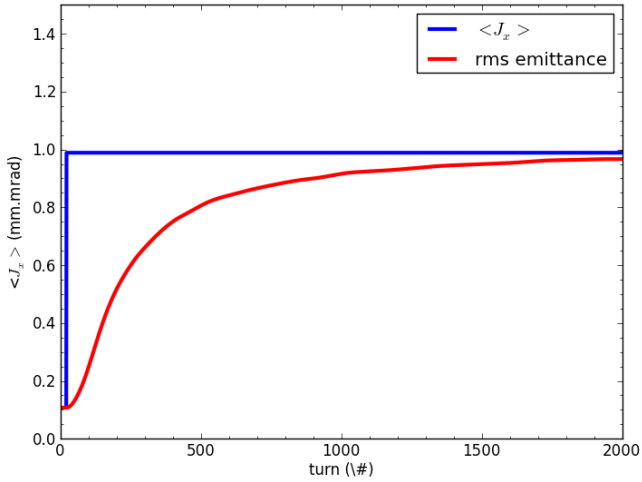

Fig. 13: The evolution of the emittance versus turn using the definition of mean action as well as rms-emittance for an injection steering error in the presence of non-linear fields where the beam distribution is filamenting.

The principal behind a transverse feedback is illustrated in Fig. 16. The trajectory excursion is measured with one or more beam position monitor(s) at a certain position along the ring and the required correction is calculated in a processing unit and sent to a fast transverse kicker that will correct the trajectory error with respect to the orbit. Depending on the bandwidth of the system even bunch-by-bunch up to intra-bunch oscillations can be damped in this manner. The result of the action of a transverse feedback on the injection error and the resulting injection oscillations is shown in Fig. 17 and the effect on the emittance in Fig. 18. The emittance will nevertheless grow in the presence of a transverse damper as it can only correct the oscillations with limited gain. The reduction in growth with respect to the situation without damper depends on the ratio of filamentation time τ_{DC} and damping time

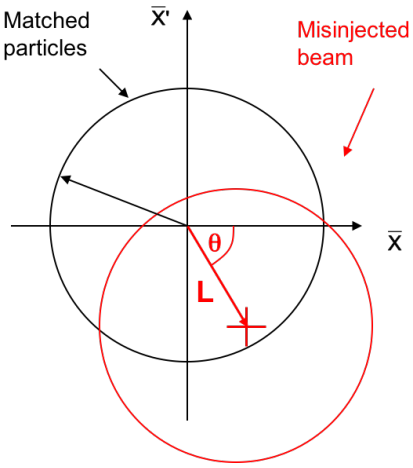

Fig. 14: The misinjected beam is offset in normalised phase space by $L = \Delta a\sqrt{\varepsilon}$ with respect to the matched distribution.

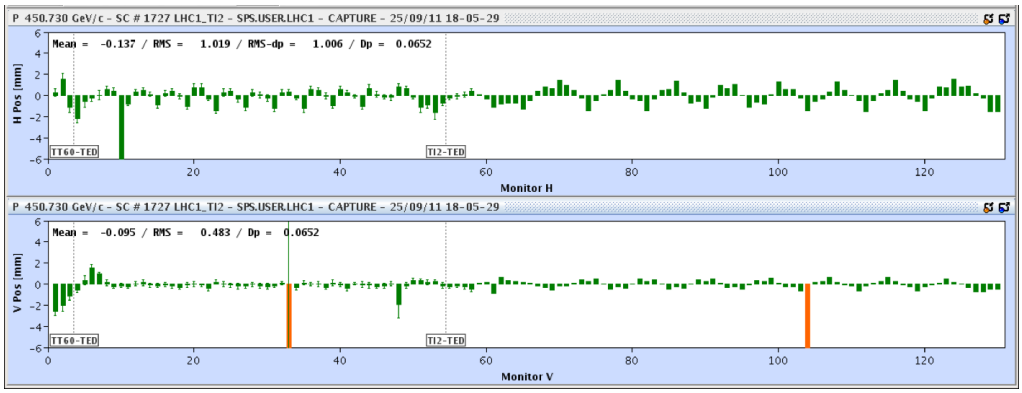

Fig. 15: A screen shot of the injection oscillation display for LHC beam 1. It shows the transfer line trajectory in the horizontal and vertical plane for the transfer between the LHC injector and the LHC itself, as well as the first turn at the pick ups of the first 3 km in the LHC minus the closed orbit at injection energy. The plot spans 6 km.

τ_d of the feedback system. The emittance blow-up for injection error Δx and $\Delta x'$ in the presence of a transverse feedback is [4]

$$\frac{\varepsilon}{\varepsilon_0} = 1 + \frac{1}{2}\frac{\Delta x^2 + (\beta\Delta x' + \alpha\Delta x)^2}{\beta\varepsilon_0}\left(\frac{1}{1+\tau_{DC}/\tau_d}\right)^2 . \tag{18}$$

3.2 Emittance blow-up from betatron mismatch

Optical errors can occur in the transfer line and the ring, such that the beam can be injected with a mismatch. The shape of the injected beam then corresponds to different twiss parameters α and β than the closed solution of the ring at the injection point. At the moment of injection the area of the particle distribution in phase space might be the same as for the desired matched distribution, see Fig. 19, only the orientation is different. Filamentation will introduce an emittance increase. The coordinates of the

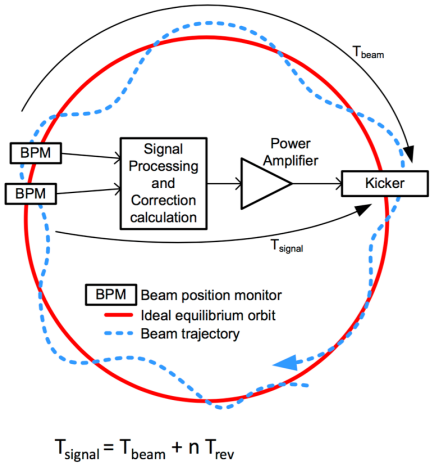

Fig. 16: The principle of the transverse feedback system: the trajectory excursion is measured with one or more beam position monitor(s) at a certain position along the ring and the required correction is calculated in a processing unit and sent to a fast transverse kicker that will correct the trajectory error with respect to the orbit.

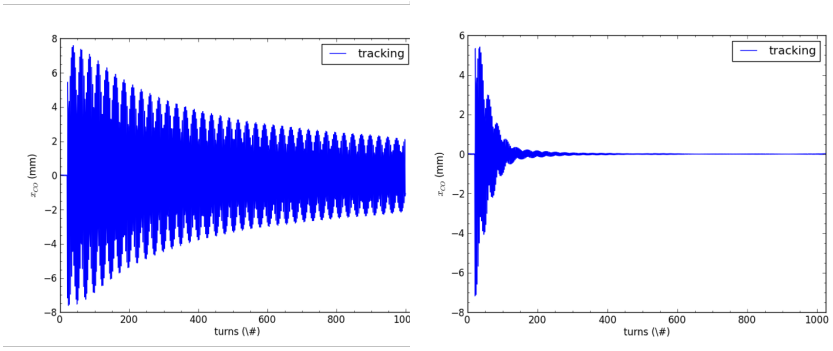

Fig. 17: The result of the action of a transverse feedback on the injection error and the resulting injection oscillations: the left plot shows the injection oscillations without transverse feedback and the left plot with. The damping time is faster than the filamentation time.

particles on the injected ellipse are

$$\begin{aligned} x_2 &= \sqrt{2\beta_2 J_x}\cos\phi \\ x_2' &= -\sqrt{\tfrac{2J_x}{\beta_2}}(\sin\phi + \alpha_2\cos\phi)\,. \end{aligned} \tag{19}$$

Transforming the coordinates in Eq. (19) to the normalised phase space defined by the matched twiss parameters α_1, β_1 results in an ellipse in normalised phase space and not a circle.

$$\begin{pmatrix} \overline{x_2} \\ \overline{x_2}' \end{pmatrix} = \sqrt{\frac{1}{\beta_1}} \cdot \begin{pmatrix} 1 & 0 \\ \alpha_1 & \beta_1 \end{pmatrix} \cdot \begin{pmatrix} x_2 \\ x_2' \end{pmatrix}\,. \tag{20}$$

The ellipse is defined by

$$2J_x = \overline{x}_2^2[\frac{\beta_1}{\beta_2} + \frac{\beta_2}{\beta_1}(\alpha_1 - \alpha_2\frac{\beta_1}{\beta_2})^2] + \overline{x'}_2^2\frac{\beta_2}{\beta_1} - 2\overline{x}_2\overline{x}_2'[\frac{\beta_2}{\beta_1}(\alpha_1 - \alpha_2\frac{\beta_1}{\beta_2})]\,, \tag{21}$$

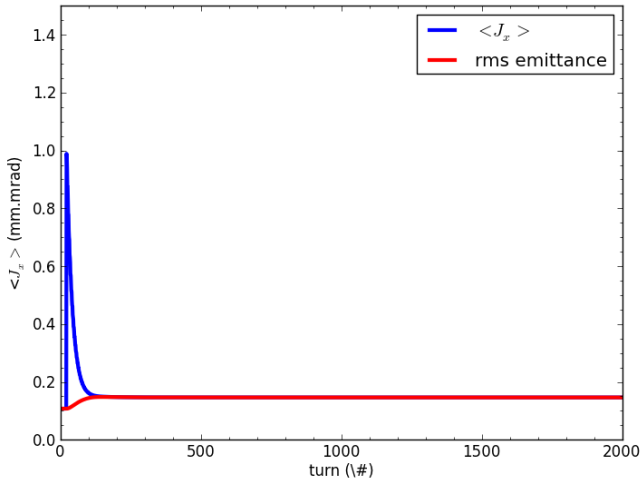

Fig. 18: The evolution of the emittance versus turn for an injection steering error using the definition of mean action as well as rms-emittance in the presence of non-linear fields and transverse feedback system. The final emittance blow-up depends on the ratio of filamentation time versus damping time τ_{DC}/τ_d.

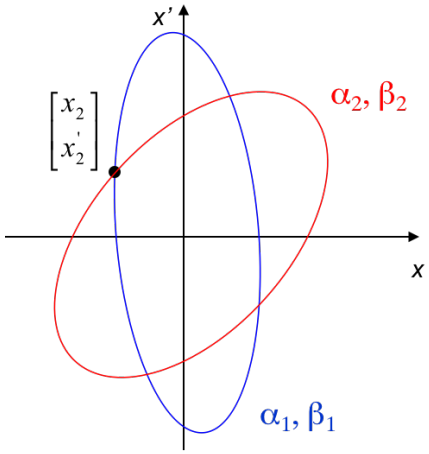

Fig. 19: Betatron mismatch illustrated in real phase space. The blue ellipse represents the matched twiss parameters (α_1, β_1), the injected beam (red curve) arrives however on an ellipses describing different twiss parameters (α_2, β_2).

which can be characterised by γ_{new}, β_{new} and α_{new} following Eq. (11):

$$\begin{aligned} \alpha_{new} &= -\frac{\beta_2}{\beta_1}(\alpha_1 - \alpha_2\frac{\beta_1}{\beta_2}) \\ \beta_{new} &= \frac{\beta_2}{\beta_1} \\ \gamma_{new} &= \frac{\beta_1}{\beta_2} + \frac{\beta_2}{\beta_1}(\alpha_1 - \alpha_2\frac{\beta_1}{\beta_2})^2 \,. \end{aligned} \tag{22}$$

From the general ellipse properties [5], the parameters a, b and λ can be introduced (Fig. 20), where a and b are the half axes of the ellipse which are related to the radius of the matched circle $A = \sqrt{2J}$ via

$$\begin{aligned} a &= A/\lambda \\ b &= A \cdot \lambda \end{aligned} \tag{23}$$

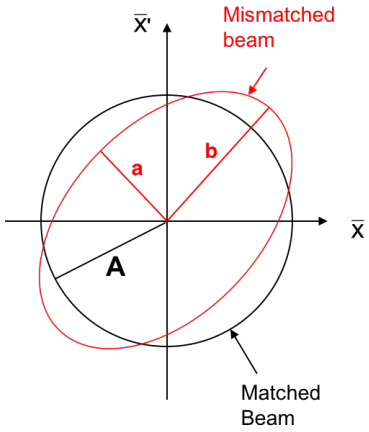

Fig. 20: Betatron mismatch in normalised phase space: The mismatched beam is enclosed by an ellipse. The half axes of the ellipse are related to the matched circle of same area with $a = A/\lambda$ and $b = A \cdot \lambda$.

and

$$\begin{aligned} a &= \tfrac{A}{\sqrt{2}}(\sqrt{H+1}+\sqrt{H-1}) \\ b &= \tfrac{A}{\sqrt{2}}(\sqrt{H+1}-\sqrt{H-1}) \end{aligned} \tag{24}$$

where

$$H = \frac{1}{2}(\gamma_{new}+\beta_{new}) = \frac{1}{2}(\frac{\beta_1}{\beta_2}+\frac{\beta_2}{\beta_1}(\alpha_1-\alpha_2\frac{\beta_1}{\beta_2})^2+\frac{\beta_2}{\beta_1}) \tag{25}$$

such that

$$\begin{aligned} \lambda &= \tfrac{1}{\sqrt{2}}(\sqrt{H+1}+\sqrt{H-1}) \\ \tfrac{1}{\lambda} &= \tfrac{1}{\sqrt{2}}(\sqrt{H+1}-\sqrt{H-1})\,. \end{aligned} \tag{26}$$

The coordinates of the mismatched distribution in normalised phase space at the injection point can then be written simply as

$$\begin{aligned} \overline{x}_{new} &= \lambda \cdot A\sin(\phi+\phi_1) \\ \overline{x}'_{new} &= \tfrac{1}{\lambda} \cdot A\cos(\phi+\phi_1)\,. \end{aligned} \tag{27}$$

After filamentation the particles' trajectories will be circles concentric to the circle of the matched distribution. The equation of the circle for one particular particle with the new coordinates is

$$2J_{new} = \overline{x}^2_{new} + \overline{x}'^2_{new} = \lambda^2 \cdot 2J_0\sin^2(\phi+\phi_1) + \frac{1}{\lambda^2}2J_0\cos^2(\phi+\phi_1)\,. \tag{28}$$

The emittance after filamentation is again the average over all phases, where we use that $\langle\sin^2(\phi+\phi_1)\rangle = \langle\cos^2(\phi+\phi_1)\rangle = 1/2$

$$\begin{aligned} \varepsilon_{new} = \langle J_{new}\rangle &= \tfrac{1}{2}(\lambda^2\langle 2J_0\sin^2(\phi+\phi_1)\rangle + \tfrac{1}{\lambda^2}\langle 2J_0\cos^2(\phi+\phi_1)\rangle) \\ &= \langle J_0\rangle(\lambda^2\langle\sin^2(\phi+\phi_1)\rangle + \tfrac{1}{\lambda^2}\langle\cos^2(\phi+\phi_1)\rangle) \\ &= \tfrac{1}{2}\varepsilon_0(\lambda^2+\tfrac{1}{\lambda^2})\,. \end{aligned} \tag{29}$$

For the final result λ can be substituted with the twiss parameters of the matched and the mismatched distribution:

$$\varepsilon_{new} = \frac{1}{2}\varepsilon_0(\lambda^2+\frac{1}{\lambda^2}) = H\cdot\varepsilon_0 = \frac{1}{2}\varepsilon_0(\frac{\beta_1}{\beta_2}+\frac{\beta_2}{\beta_1}(\alpha_1-\alpha_2\frac{\beta_1}{\beta_2})^2+\frac{\beta_2}{\beta_1}) \tag{30}$$

where subscript 1 refers to the matched ellipse and 2 to the mismatched one.

An example of a turn-by-turn profile measurement with betatron mismatch is shown in Fig. 21. Before the beam has fully filamented, the beam size measured by the instrument is oscillating indicating mismatch.

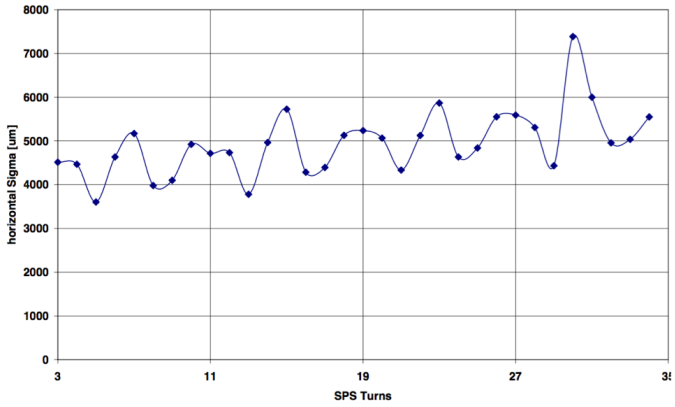

Fig. 21: Measurement of beam size versus turn after injection in the horizontal plane measured with a turn-by-turn profile monitor. The oscillation of the beam size indicates mismatch. The slope of the curve is due to emittance growth from the scattering in the foil [6].

3.3 Emittance blow-up from thin scatterer

It is sometimes necessary to have thin scatterers in the beam as thin beam screens of Al_2O_3 or Ti used to generate beam profile measurements, metal windows used to separate vacuum of transfer lines from vacuum in circular machines or foils to strip electrons to change charge state. The emittance of the beam that passes through will increase due to multiple Coulomb scattering. The rms angle increase from

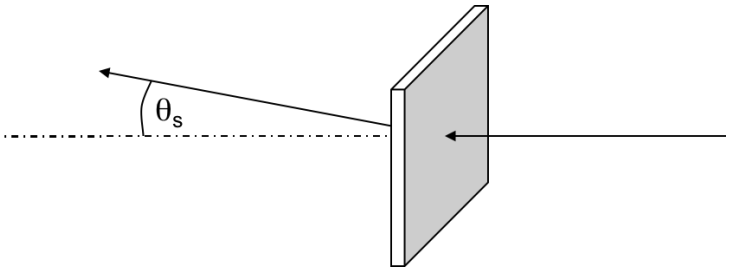

Fig. 22: The emittance of the beam that passes through a thin foil will increase due to multiple Coulomb scattering

multiple Coulomb scattering is

$$\sqrt{\langle\Theta_s^2\rangle}[mrad] = \frac{14.1}{\beta_c p[MeV/c]} Z_{inc}\sqrt{\frac{L}{L_{rad}}}(1 + 0.11 \cdot log_{10}\frac{L}{L_{rad}}) \,, \tag{31}$$

where $\beta_c = v/c$, p is the momentum, Z_{inc} is the particle charge, L the target length, and L_{rad} the radiation length of the target. Each particle gets a random change in angle Θ_s, but there is no effect on the positions at the scatterer, Fig. 23. So, the coordinates in normalised phase space at the scatterer location will transform to

$$\begin{aligned} \overline{x}_{new} &= \overline{x}_0 \\ \overline{x}'_{new} &= \overline{x}'_0 + \sqrt{\beta}\Theta_s \,. \end{aligned} \tag{32}$$

And after filamentation the particles will have an emittance $\varepsilon = \langle J_{new}\rangle$ as illustrated in Fig. 24. The action for one of the scattered particles will be

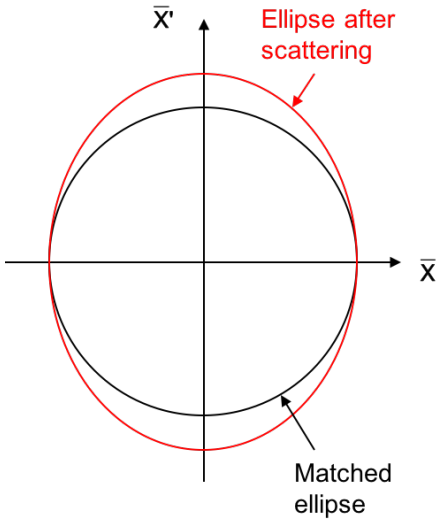

Fig. 23: Each particle gets a random angle change Θ_s, but there is no effect on the positions at the scatterer

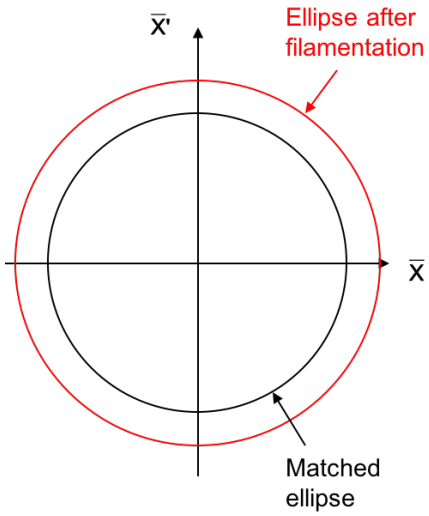

Fig. 24: Filamentation further increases the area in phase space the beam is occupying, after the increase in the angular distribution at the scatterer.

$$\begin{aligned} 2J_{new} &= \bar{x}_{new}^2 + \bar{x}_{new}'^2 \\ &= \bar{x}_0^2 + (\bar{x}_0' + \sqrt{\beta}\Theta_s)^2 \\ &= \bar{x}_0^2 + \bar{x}_0'^2 + 2\sqrt{\beta}(\bar{x}_0'\Theta_s) + \beta\Theta_s^2 \end{aligned} \tag{33}$$

and the mean action therefore, where we use that the initial angle and scattering angle are uncorrelated and the average angle $\langle \bar{x}_0' \rangle = 0$,

$$\begin{aligned} 2\langle J_{new} \rangle &= \langle \bar{x}_0^2 \rangle + \langle \bar{x}_0'^2 \rangle + 2\sqrt{\beta}\langle \bar{x}_0'\Theta_s \rangle + \beta\langle \Theta_s^2 \rangle \\ &= 2\varepsilon_0 + 2\sqrt{\beta}\langle \bar{x}_0' \rangle \langle \Theta_s \rangle + \beta\langle \Theta_s^2 \rangle \\ &= 2\varepsilon_0 + \beta\langle \Theta_s^2 \rangle \,. \end{aligned} \tag{34}$$

The new emittance after filamentation and after having traversed a thin scatterer will be

$$\varepsilon_{new} = \varepsilon_0 + \frac{\beta}{2}\langle\Theta_s^2\rangle\,. \tag{35}$$

In order to reduce the blow-up from stripping foils and other thin scatterers, they have to be placed at locations with small β-function. A small β-function means a large spread in angles, so the additional scattering angle has a small effect on the distribution. An example for the optics design of the insertion in a transfer line with a stripper foil for LHC ion transfer between the PS and SPS accelerator is shown in Fig. 25. For LHC heavy ions, Pb^{54+} is stripped to Pb^{82+} at 4.25 GeV/u using a 0.8 mm thick Al

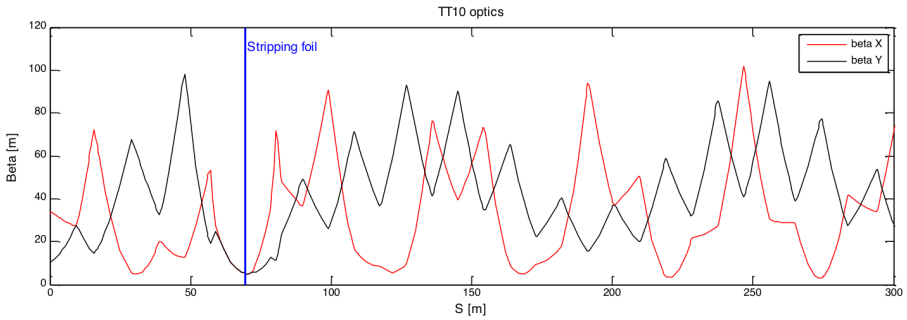

Fig. 25: This figure shows the optics in the transfer line between the accelerators PS and SPS at CERN for the LHC heavy ions. The stripper foil is located at a location with $\beta_{x,y} \approx 5$ m.

foil, in the PS to SPS line. The emittance blow-up is minimised with a low-β insertion ($\beta_{x,y} \approx 5$ m) in the transfer line. Using the formulae from above, the expected emittance blow-up is nevertheless 8%.

3.4 Emittance blow-up from other effects

The techniques that were introduced in the previous sections can be applied to various other effects and errors at injection to calculate the emittance blow-up. In the following results of some of these derivations are summarised.

3.4.1 Dispersion mismatch

In case of a dispersion mismatch by ΔD and $\Delta D'$ and a momentum spread of $\frac{\delta p}{p}$ of the beam, the emittance blow-up will be

$$\frac{\varepsilon}{\varepsilon_0} = 1 + \frac{1}{2}\frac{\Delta D^2 + (\beta\Delta D' + \alpha\Delta D)^2}{\beta\varepsilon_0}(\frac{\delta p}{p})^2\,. \tag{36}$$

3.4.2 Energy mismatch

With dispersion at the injection point and a momentum offset of the beam of $\Delta p/p$, the emittance blow-up will amount to

$$\frac{\varepsilon}{\varepsilon_0} = 1 + \frac{1}{2}\frac{D^2}{\beta\varepsilon_0}(\frac{\Delta p}{p})^2\,. \tag{37}$$

3.4.3 Geometrical mismatch

In case there is a tilt angle Θ between the beam reference systems of the injected beam and the ring at the injection point, cross-plane coupling will occur and through filamentation emittance blow-up. The

following formula gives the result in the horizontal plane [7, 8]

$$\varepsilon_x = \varepsilon_{0x}\cos^2\Theta + \frac{1}{2}\varepsilon_{0y}\sin^2\Theta \cdot \left(\frac{\beta_y}{\beta_x}(1+\alpha_x^2) + \frac{\beta_x}{\beta_y}(1+\alpha_y^2) - 2\alpha_x\alpha_y\right) . \tag{38}$$

3.5 Summary

In this lecture the generic method to calculate emittance growth from mismatch at injection was introduced. The method was applied for the most prominent injection errors and important formulae were derived. At the end of the lecture a collection of formulae for various other typical injection errors was given.

References

[1] A. Wolski, *Beam Dynamics in High Energy Particle Accelerators*, (Imperial College Press, London, 2014), https://doi.org/10.1142/p899.

[2] B. Goddard, Transfer Lines, CAS, 2004.

[3] P. Bryant, in Proceedings of the CAS-CERN Accelerator School: General Accelerator Physics, v.2, Gif-sur-Yvette, France, 3-14 September 1984, edited by P.J. Bryant and S. Turner, CERN-85-19-V-2 (CERN, Geneva, 1985), pp. 358-376, https://doi.org/10.5170/CERN-1985-019-V-2.

[4] L. Voss, Transverse emittance blow-up from double errors in proton machines, CERN, 1998.

[5] C. Bovet et al., A selection of formulae and data useful for the design of A.G. synchrotrons, 1970, CERN.

[6] G. Arduini et al., Mismatch Measurement and Correction Tools for the PS-SPS Transfer of the 26 GeV/c LHC Beam, 1999, CERN.

[7] B. Goddard et al., Expected emittance growth and beam tail repopulation from errors at injection into the LHC, IPAC proceedings, 2005.

[8] K. Fuchsberger et al., Coupling at injection from tilt mismatch between the LHC and its transfer lines, 2009, CERN.